Journal of Materials Chemistry A

Accepted Manuscript

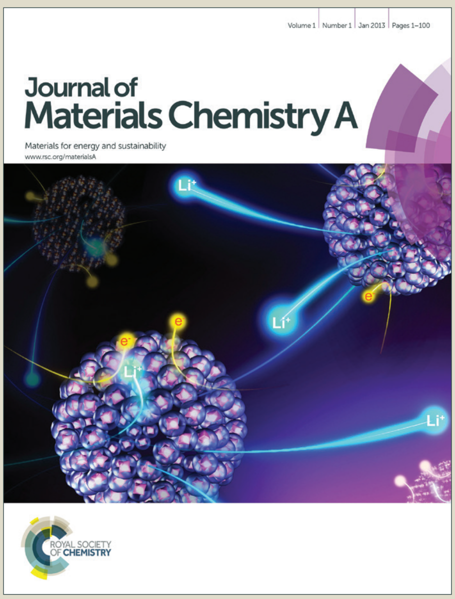

ROYAL SOCIETY OF CHEMISTRY

www.rsc.org/materialsA

Journal of
Materials Chemistry A

RSCPublishing

ARTICLE

Synthesis and Evaluation of Porous Azo-Linked Polymers for Carbon Dioxide Capture and Separation

Cite this: DOI: 10.1039/x0xx00000x

Received 00th January 2012,
Accepted 00th January 2012

DOI: 10.1039/x0xx00000x

www.rsc.org/

Pezhman Arab, Emily Parrish, TimurIslamoglu, and Hani M. El-Kaderi*

A series of new azo-linked polymers (ALPs) was synthesized via copper(I)-catalyzed oxidative homocoupling of 2D and 3D aniline-like monomers. ALPs have moderate surface areas (SA_{BET} = 412-801 m^2 g^{-1}), narrow pore sizes (□ 1nm), and high physiochemical stability. The potential applications of ALPs for selective CO_2 capture from flue gas and landfill gas at ambient temperature were studied. ALPs exhibit high isosteric heats of adsorption for CO_2 (28.6-32.5 kJ mol^{-1}) and high CO_2 uptake capacities of up to 2.94 mmol g^{-1} at 298 K and1 bar. Ideal adsorbed solution theory (IAST) selectivity studies revealed that ALPs have good CO_2/N_2(56) and CO_2/CH_4(8) selectivities at 298 K. The correlation between the performance of ALPs in selective CO_2 capture and their properties such as surface area, pore size, and heat of adsorption was investigated. Moreover, the CO_2 separation ability of ALPs from flue gas and landfill gas under pressure-swing adsorption (PSA) and vacuum-swing adsorption (VSA) processes were evaluated. The results show that ALPs have promising working capacity, regenerability, and sorbent selection parameter values for CO_2 separation by VSA and PSA processes.

1 Introduction

Design and synthesis of porous organic polymers (POPs) have recently attracted tremendous interest due to the high surface area, tunable chemical functionality, and remarkable physicochemical stability of this class of materials.[1-2] The synthesis of POPs featuring Lewis basic functionalities is of particular interest since this enables selective CO_2 capture from gas mixtures.[3] As fossil fuels remain the primary source of energy, anthropogenic CO_2 emissions to the atmosphere have risen dramatically which has resulted in global warming in a very short period of time.[4] Therefore, CO_2 capture and sequestration (CCS) has been proposed as a medium-term solution until renewable clean energy sources become widely accessible.[3] CO_2 capture by aqueous amine solutions is currently the most widely used technology in industry for removal of CO_2 from gas mixtures.[5] In this process, aqueous amine solutions chemically react with CO_2, and therefore sorbent regeneration is energy-intensive.[5] Furthermore, this process suffers from other drawbacks such as solvent decomposition, corrosiveness, toxicity, and volatility.[5-6] To address these limitations, physisorption of CO_2 by porous adsorbents such as metal organic frameworks (MOFs), porous carbons, and POPs has received significant attention as a promising alternative method.[7]The physisorption of CO_2 takes place via relatively weak van der Waals interactions between CO_2 and porous adsorbents, making the regeneration processes more energy efficient.[3, 7-8]

Very recently, azo-linked POPs have emerged as a new class of CO_2adsorbents with exceptional physicochemical stability and high CO_2 uptake capacity.[9-12]Both theoretical[13] and experimental[9-10] studies have shown that porous frameworks functionalized with azo groups exhibit high CO_2 uptake capacity and/or selectivity due to Lewis acid-base interactions between CO_2 and azo groups. In addition, the photo-responsive nature of the azo-linkage could be utilized for CO_2 release via *trans-to-cis* isomerization by UV.[14]Patel *et al.*have recently reported very high CO_2/N_2 selectivity values (up to 131 at 298

K) for azo-linked covalent organic polymers (azo-COPs); however, the low porosity of azo-COPs resulted in modest CO_2 uptake capacities (1.2 - 1.5 mmol g^{-1}, 298 K and 1 bar) which could limit their applications in CO_2 capture.[10] To address this drawback, we have introduced a facile synthetic route for the synthesis of highly porous azo-linked polymers (ALPs) with remarkable CO_2 uptake capacities of up to 3.2 mmol g^{-1} (298 K and 1 bar).[9] However, the CO_2/N_2 selectivities of ALPs (26-35 at 298K) are much lower than those of azo-COPs (96-131 at 298 K).[9] ALPs[9] have higher surface area, greater pore volume, and larger pore width than azo-COPs[10] which affect their performance in selective CO_2 capture.[9] Azo-linked polymers with different structural properties (pore size, surface area, and pore volume) can be synthesized from diverse building units and different synthetic routes.[9-11] Therefore, it is necessary to investigate the dependence of CO_2separation ability of azo-linked polymers on their structural properties. To be practical, a porous sorbent must be highly selective toward CO_2 and also have high CO_2 uptake capacity[3, 15]; however, all previously reported azo-linked porous polymers might only meet one of these criteria at best.[9-10] Accordingly, design and synthesis of new azo-linked POPs should be aimed at achieving both high CO_2uptake capacity and selectivity simultaneously. Moreover, CO_2 uptake capacity and selectivity do not provide enough information for evaluation of a sorbent's effectiveness since they do not consider the cyclic nature of CO_2 separation processes.[16-17] Therefore, other critical criteria such as regenerability, working capacity, and sorbent selection parameters should also be evaluated for comprehensive assessment of CO_2 sorbents in a cyclic separation process.[16-17] Pressure-swing adsorption (PSA) and vacuum-swing adsorption (VSA) processes are now used as efficient technologies for regeneration of adsorbents for a number of applications.[16] In a PSA or VSA process, after adsorption takes place, the adsorbent is regenerated by desorption of CO_2under a reduced pressure without applying heat.[17] In a PSA process, CO_2 is adsorbed from a gas mixture at a high pressure (>1 bar), and the regeneration takes place upon reducing the pressure to 1 bar. On the other hand, in a VSA process, the adsorption pressure is ~ 1 bar, and the adsorbent is regenerated by reducing the pressure to ~ 0.1 bar.

With these considerations in mind, we applied new nitrogen-rich building units to synthesize new ALPs in an attempt to combine both high CO_2 uptake capacity and selectivity. One of the polymers, ALP-5, was successful in meeting both of these criteria simultaneously. Moreover, the new ALPs were evaluated for selective CO_2 removal from flue gas and landfill gas under PSA and VSA processes. Our study highlights the influence of properties (surface area, pore size, and heat of adsorption) of azo-linked polymers on their CO_2 separation ability. We demonstrate that the optimization of such variables can lead to remarkable CO_2 capturing properties fort his class of porous organic polymers.

2 Experimental section

2.1 Materials and methods

All chemicals were purchased from commercial suppliers (Acros Organics, Sigma Aldrich, or Frontier Scientific) and used without further purification, unless otherwise noted. N,N,N′,N′,tetrakis(4-aminophenyl)-1,4-phenylenediamine(TAPPA) was purchased from Combi-Blocks. 2,2′,7,7′-Tetraamino-9,9′-spirobifluorene[18] (TASBF), tris(4-aminophenyl)amine[19] (TAPA), and 1,1,2,2-tetrakis(4-aminophenyl)ethene[20](TAPE) were synthesized according to literature procedures. Solid-state ^{13}C cross-polarization magic angle spinning (CP-MAS) NMR spectra of polymers were taken at Spectral Data Services, Inc. Elemental analyses were performed by Midwest Microlab LLC. Thermogravimetric analysis (TGA) was carried out by a Perkin-Elmer Pyris 1 thermogravimetric analyzer under a nitrogen atmosphere with a heating rate of 10 °Cmin^{-1}. For Scanning Electron Microscopy (SEM) imaging, the samples were prepared by dispersing each polymer onto the surface of a sticky carbon attached to a flat aluminum sample holder. Then, the samples were coated with platinum at a pressure of 1×10^{-5} mbar in a N_2 atmosphere for 60 seconds before SEM imaging. The images were taken by a Hitachi SU-70 scanning electron microscope. Powder X-ray diffraction patterns were obtained by using a Panalytical X'pert pro multipurpose diffractometer (MPD) with Cu Kα radiation. FT-IR spectra of the samples were obtained by a Nicolet-Nexus 670 spectrometer having an attenuated total reflectance accessory.Low pressure gas sorption measurements were carried out by a Quantachrome Autosorb iQ volumetric analyzer using UHP grade adsorbates. High pressure gas sorption measurements were performed using a VTI HPVA-100 volumetric analyzer. High pressure total gas uptakes were calculated according to literature methods using NIST Thermochemical Properties of Fluid Systems.[21]The samples were degassed at 120 °C under vacuum for 24 hours before gas sorption measurements.

2.2 Synthesisof polymers

Synthesis of ALP-5. This polymer was synthesized following a modified procedure described in our recent work.[9] CuBr (25 mg, 0.174 mmol) and pyridine (110 mg, 1.391 mmol) were added to 11 mL toluene. The mixture was stirred at 25 °C for 3 h in an open air atmosphere. The resulting mixture was added to a solution of 2,2′,7,7′-tetraamino-9,9′-spirobifluorene (100 mg, 0.266 mmol) in 11 mL THF. The mixture was stirred in an open air atmosphere at 25 °C for 24 h, at 60 °C for 12 h, and then at 80 °C for 12 h. The resulting brownish solid was isolated by filtration over a medium glass frit funnel and subsequently washed with THF and water. The obtained powder was stirred in HCl (100 mL, 2 M) for 12 h, then filtered and washed with water. The powder was further washed with NaOH (2 M), water, ethanol, THF, and chloroform. Finally, the obtained product was dried at 120 ºC under vacuum (150mTorr) to give ALP-5 as a brownish fluffy powder (79 mg, 81%). Elemental analysis calcd. (%) for $C_{25}H_{12}N_4$: C, 81.51; H, 3.28; N, 15.21. Found (%): C,74.88; H, 3.86; N, 13.34.

Synthesis of ALP-6. This polymer was synthesized by following the same synthetic method described above for ALP-5 using N,N,N′,N′-tetrakis(4-aminophenyl)-1,4-phenylenediamine (100 mg, 0.212 mmol), CuBr (40 mg, 0.279 mmol), and pyridine (160 mg, 2.023mmol).The final product was obtained as a brown powder which was denoted as ALP-6 (88 mg, 90%). Elemental analysis calcd. (%) for $C_{30}H_{20}N_6$: C, 77.57; H, 4.34; N, 18.09. Found (%): C, 69.52; H, 4.18; N, 14.66.

Synthesis of ALP-7. This polymer was prepared following the same method described above for ALP-5 using tris(4-aminophenyl)amine (100 mg, 0.344 mmol), CuBr (40 mg, 0.279 mmol), and pyridine (160 mg, 2.023 mmol). The final product was obtained as a brownish powder, denoted as ALP-7 (85 mg, 87%). Elemental analysis calcd. (%) for $C_{18}H_{12}N_4$: C, 76.04; H, 4.25; N, 19.71. Found (%): C, 71.07; H, 4.20; N, 16.46.

Synthesis of ALP-8. This polymer was synthesized following the synthetic method described above for ALP-5 using 1,1,2,2-tetrakis(4-aminophenyl)ethane (100 mg, 0.255 mmol), CuBr (25 mg, 0.174 mmol) and pyridine (110 mg, 1.391 mmol). The final product was obtained as a brown powder, denoted as ALP-8 (77 mg 79%). Elemental analysis calcd. (%) for $C_{26}H_{16}N_4$: C, 81.23; H, 4.20; N, 14.57. Found (%): C, 74.36; H, 4.47; N, 12.60.

3 Results and discussion

3.1 Synthesis and characterization of ALPs

The synthesis of ALPs was carried out according to our previously reported procedure via oxidative homocoupling reaction of aniline-like monomers that leads to azo bond formation as depicted in Scheme 1.[9]The monomers used for the synthesis of new ALPs were selected based on the topology-directed approach developed for preparation of POPs using rigid star-shaped monomers.[1] A recent study has shown that the incorporation of tertiaryamines into POPs can result in enhanced CO_2/N_2 selectivities.[22] Therefore, we used tertiaryamine-based monomers for the synthesis of ALP-6 and ALP-7 in an attempt to achieve high selectivity values.It is worth noting that the synthesis of ALP-7 using the same amount of catalyst reported in our recent work[9] resulted in low surface area of 60 m^2 g^{-1} (entry 1 in Table S1). This could be attributed to incomplete polymerization caused by low activity of the CuBr-pyridine catalyst due to coordination of the tertiaryamine of the monomer to copper cations. In fact, doubling the amount of catalyst resulted in much higher surface area of 400 m^2 g^{-1}(entry 2 in Table S1). Further increase in catalyst amount led to a low surface area of 100 m^2 g^{-1} (entry 3 in Table S1). This can be attributed to afast polymerization rate which results in higher degree of framework interpenetration.[23]Since the monomer used for synthesis of ALP-6 contains tertiary amine, the synthesis of ALP-6 was

Scheme 1. Synthesis of azo-linked porous polymers (ALPs).Reaction conditions: CuBr, pyridine, THF/toluene (25-80 °C, 48 h).

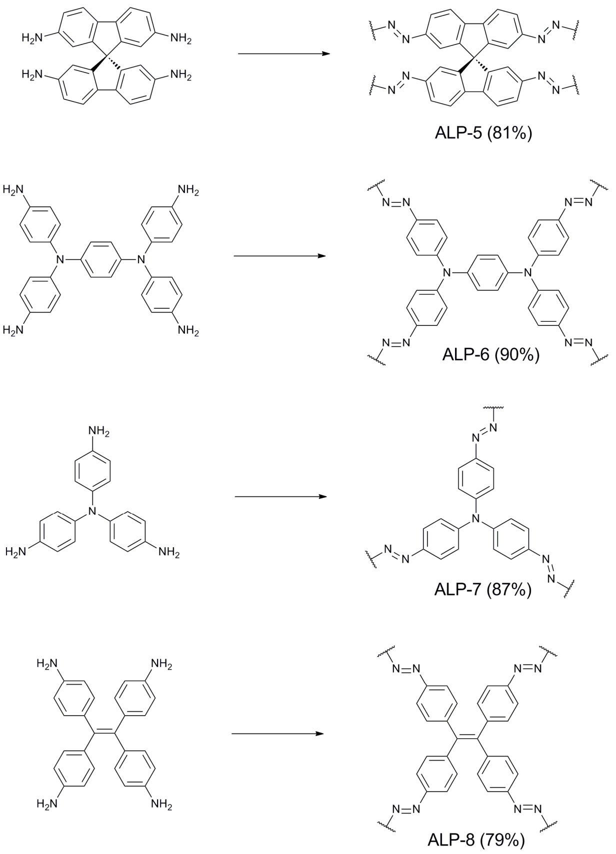

carried out using the synthetic conditions optimized for ALP-7.FTIR studies reveal the successful polymerization of monomers by appearance of characteristic bands for N=N vibrations at 1415-1400 cm^{-1} (Fig. S1-S4).[9-10]Upon polymerization, the intensity of the band resulting from N-H stretches (3200-3450 cm^{-1}) significantly decreased (Fig. S1-S4). The residual signals at this region can be attributed to the presence of terminal amines on the surface of ALPs' particles. In addition, ^{13}C CP-MAS NMR spectra of ALPs were collected to confirm the expected structures of ALPs (Fig. S5-S8). All ALPs are insoluble in organic solvents such as DCM, DMF, THF, and DMSO, showing their expected hyper-cross-linked networks.[24]Elemental analysis studies of ALPs show some deviations from expected values for hypothetical networks. These deviations are common for POPs, and are mainly attributed to incomplete polymerization as well as adsorption of moisture during handling.[9, 25]SEM images of ALPs show aggregated spherical particles of variable size (200-800 nm) as shown in Fig. S9-S12.The XRD patterns of ALPs are featureless (Fig. S13), indicating their amorphous structure which is caused by the rapid and irreversible formation of the azo linkage.[26]Thermogravimetric analysis (TGA) shows that ALPs are stable up to ~400 °Cunder nitrogen while initial

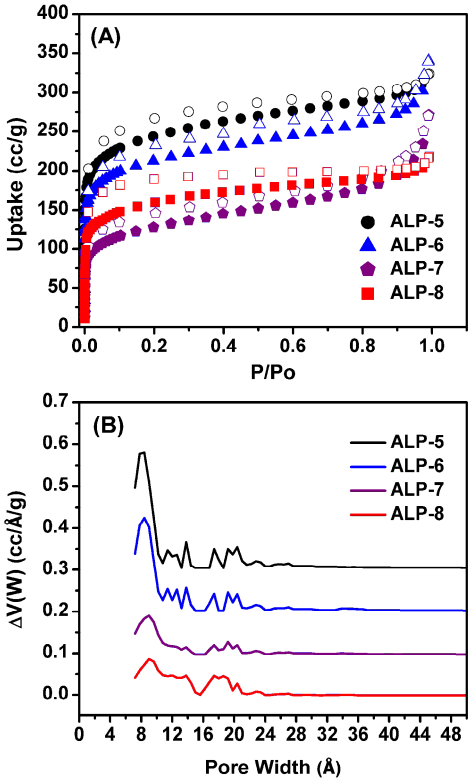

Fig. 1 Ar uptake isotherms (A) and pore size distributions (B) of ALPs. Filled and open symbols represent adsorption and desorption, respectively. For clarity, pore size distributions of ALP-5, ALP-6, and ALP-7 are offset by 0.3, 0.2, and 0.1 respectively.

weight loss below 100 °Ccan be attributed to desorption of adsorbed moisture (Fig. S14).

It should also be noted that porous azo-linked polymers have high chemical stability toward water.[10, 12]To study the water stability of ALPs, their surface areas were measured after they were stirred in boiling water for 48 h. No noticeable change in surface areas was observed, indicating the high water stability of ALPs. It is noteworthy that ALPs have high chemical stability in acidic (2 M HCl) and basic (2 M NaOH) conditions.

3.2 Porosity measurements and CO_2 uptake studies

The porosity of ALPs was studied by Ar adsorption isotherms collectedat 87 K as shown in Fig. 1A.All Ar adsorption isotherms exhibit a rapid uptake at very low relative pressures of below 0.04 due to the permanent microporosity of the polymers.[27]The gradual increase in Ar uptake at higher relative pressures (0.04-0.9) can be attributed to thepresence of a small portion of mesoporosity.[27-28]The specific surface areas of ALPs were calculated from adsorption branch of Ar isotherms using the Brunauer-Emmett-Teller (BET) method and were found to be 801, 698, 412, and 517 m^2 g^{-1} for ALP-5, ALP-6, ALP-7, and ALP-8, respectively. The surface area of ALP-5 (801 m^2 g^{-1}) is higher than those of azo-COPs (493-729 m^2 g^{-1})[10] and azo-POFs (439-712 m^2 g^{-1})[11]but lower than those of our previously reported ALPs (862-1235 m^2 g^{-1}).[9]Pore size distributions (PSD) of ALPs were calculated from Ar adsorption branch using nonlocal density functional theory (NLDFT), and are depicted in Fig. 1B.The overall PSDs of ALPs are similar, showing a major peak centred at around 8-9 Å and broadly distributed pores below 25 Å.The total pore volumes of ALPs were estimated from single point Ar uptake at P/P_o of 0.9 and found to be 0.25–0.39 $cm^3 g^{-1}$. The porosity parameters of ALPs are summarized in Table 1.

Table 1. Porosity parameters of ALPs

Polymer	SA_{BET}[a]	Dominant Pore Size[b]	V_{total}[c]
ALP-5	801	0.80	0.39
ALP-6	698	0.85	0.36
ALP-7	412	0.90	0.27
ALP-8	517	0.92	0.25

[a]Surface area (m^2 g^{-1}) calculated from the Ar adsorption branch based on the BET model. [b]Pore size distribution (nm) estimated from the adsorption branch of the Ar isotherm using NLDFT. [c]Total pore volume (cm^3 g^{-1}) calculated from single point Ar uptake at P/P_o= 0.90.

It has been reported that microporous sorbents having pore size below 1.0 nm are very useful for CO_2 capture and separation.[29]In order to study the CO_2 uptake capacity of ALPs, single component CO_2isotherms were collected at 273 and 298 K (Fig. 2). The CO_2 isotherms of ALPs are completely reversible and exhibit a steep rise at low pressures (Fig. 2).While the steep rise at low pressures shows strong dipole-quadrupole integrations between CO_2 and azo groups of ALPs, the reversible nature of CO_2 isotherms indicates that ALPs can be readily regenerated by simply reducing the pressure at ambient temperature. ALP-5 exhibits the highest CO_2 uptake among new ALPs, reaching 4.46 and 2.94 mmol g^{-1} at 273 K and 298 K respectively (Table 2). The CO_2 uptake capacity of ALP-5 at 298 K (2.94 mmol g-1) is higher than that of azo-COPs (1.2- 1.5 mmol g^{-1})[10] and azo-POFs (1.2- 1.9 mmol g^{-1})[11] but slightly lower than that of the best performing azo-linked polymer ALP-1 (3.2 mmol g^{-1}).[9] The Q_{st} of CO_2 was calculated by the virial method and found to be 28.6-32.5 kJ mol^{-1} at zero coverage (Fig. 2 and Table 2). Notably, ALP-5 exhibits the highest value (32.5 kJ mol^{-1}) among all previously reported classes of azo-linked porous polymers, including ALPs (27.9-29.6 kJ mol^{-1})[9], azo-POFs (26.2- 27.5 kJ mol^{-1})[11], and azo-COPs (24.8-32.1 kJ mol^{-1})[10]. The higher binding affinity of ALP-5 for CO_2, when compared to other ALPs, can be attributed to its narrower pores (~8 Å), as shown in Table S2.[3, 15]

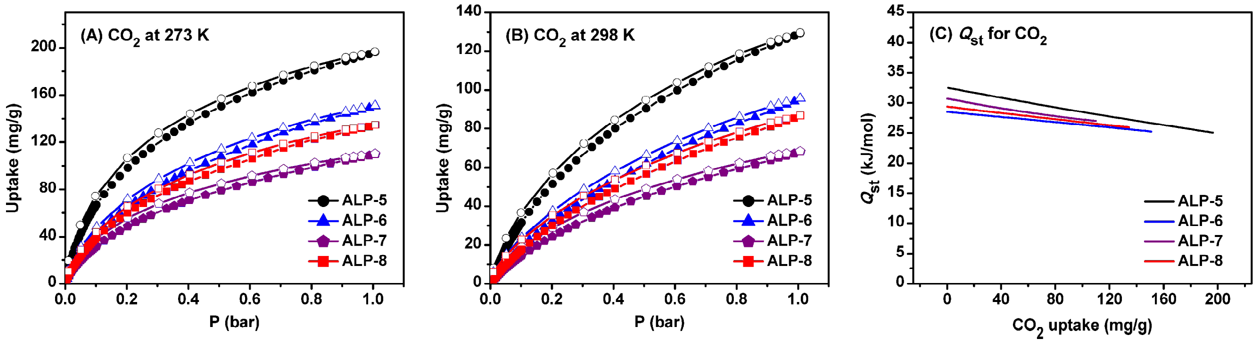

Fig. 2 CO_2 uptake isotherms for ALPs at 273 K (A) and 298 K (B), and isosteric heat of adsorption for CO_2 (C).

In general, stronger CO_2-framework interactions can be expected in POPs having narrow pores due to higher number of interactions between the adsorbed CO_2 and pore walls.[3] For the same reason, ALP-5 has the highest Q_{st} for CH_4 when compared to other ALPs (Table S3).[30] Moreover, the CO_2 uptake capacity of microporous organic polymers usually increases with surface area.[3, 9, 31] Consequently, the high CO_2 uptake capacity of ALP-5 when compared to other ALPs can be attributed to the combined effects of its narrow pores and high surface area.[32]. Despite its high nitrogen content and high Q_{st} for CO_2, ALP-7 exhibits the lowest CO_2 uptake capacity among ALPs due to its lower surface area (Table 2).[3, 16] The CO_2 uptake capacities of ALPs are compared to those of other classes of porous azo-linked polymers in Table S4. It is important to note that a high CO_2 uptake capacity at 1.0 bar does not necessarily reflect the effectiveness of the sorbent in post-combustion CO_2 capture applications since the partial pressure of CO_2 in flue gas is only ~0.1-0.15 bar.[32-35] Therefore, the CO_2 uptake capacity at low pressure is more relevant for CO_2 separation from the flue gas.[32-34] To provide a better evaluation of the new ALPs for CO_2 separation, we compared their low-pressure CO_2 uptake to that of ALP-1,which has thehighest CO_2 uptake at 1 bar among all previously reported azo-linked polymers (Fig. 3). ALP-5 exhibits CO_2 uptake capacity of 0.95 mmol g^{-1}at 0.15 bar and 298 K, outperforming all other ALPs (Fig. 3). Interestingly, although the surface area of ALP-5 (801 m^2 g^{-1}) is much lower than that of ALP-1 (1235 m^2 g^{-1}), it adsorbs more CO_2 at low pressure. This can be attributed to the higher Q_{st} value of ALP-5 for CO_2 (Table 2).[15]On the other hand, the CO_2 uptake capacity of ALP-5 at 298 K and 1.0 bar (2.94 mmol g^{-1}) is lower than that of ALP-1 (3.2 mmol g^{-1}), which indicates that the effect of surface area on CO_2 uptake capacity becomes more dominant at 1.0 bar.[15] These results show that the effect of Q_{st} on CO_2 uptake at low pressures is more significant than that of surface area; while CO_2 uptake at high pressures correlates more with surface area.[15, 36]

Table 2. Gas uptake, selectivity, and isosteric heat of adsorption for ALPs

Polymer	Surface Area[a]	CO_2 at 1.0 bar[b]			CH_4 at 1.0 bar[b]			N_2 at 1.0 bar[b]		Selectivity[c]	
		273K	298 K	Q_{st}	273 K	298K	Q_{st}	273 K	298 K	CO_2/N_2	CO_2/CH_4
ALP-1	1235	5.37	3.24	29.2	1.63	0.94	20.8	0.41	0.22	44 (28)	8 (6)
ALP-5	801	4.46	2.94	32.5	1.44	0.85	22.4	0.40	0.18	60 (47)	14 (8)
ALP-6	698	3.42	2.17	28.6	1.02	0.60	19.0	0.25	0.10	45 (48)	10 (7)
ALP-7	412	2.50	1.55	30.7	0.73	0.40	22.2	0.19	0.06	52 (56)	12 (8)
ALP-8	517	3.05	1.97	29.4	0.91	0.53	20.04	0.21	0.10	51 (44)	11 (7)

[a]Surface area (m^2 g^{-1}) calculated from the Ar adsorption branch based on the BET model. [b]Gas uptake in mmol g^{-1}, and isosteric heat of adsorption (Q_{st}) at zero coverage in kJ mol^{-1}. [c]Selectivity (mol mol^{-1}, at 1.0 bar) calculated by IAST method at mole ratio of 10:90 for CO_2/N_2, and mole ratio of 50:50 for CO_2/CH_4 at 273 K and (298 K).

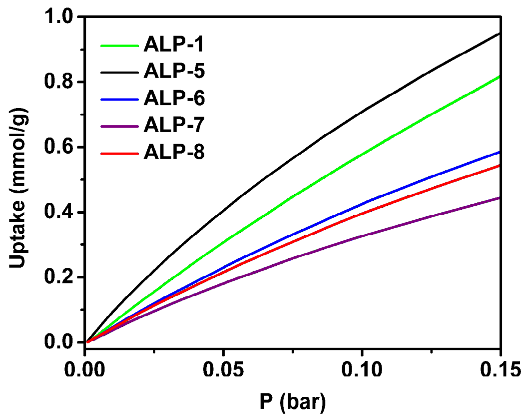

Fig. 3 Low-pressure CO_2 uptake capacity of ALPs at 298 K.

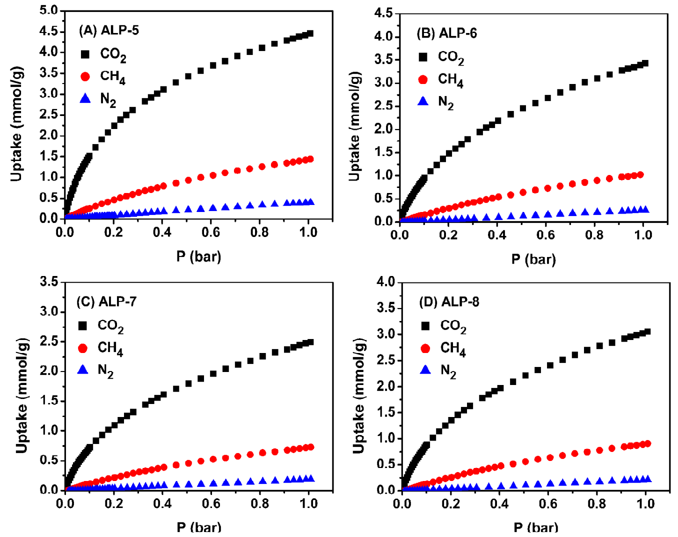

Fig. 4 CO_2, CH_4, and N_2 adsorption isotherms of ALPs at 273 K.

The CO_2 uptake capacity of ALP-7 at 0.15 bar is much lower than that ofALP-1 despite its higher Q_{st} for CO_2. This poor performance of ALP-7 for CO_2 uptake arises from its low surface area (412 $m^2\ g^{-1}$).[3, 16] Accordingly, the high CO_2 uptake of ALP-5 at low pressure can be attributed to the combined effects of its high surface area and high Q_{st} for CO_2.[16, 32]It should be noted that the unreacted terminal amine groups on the surface of ALPs' particles can contribute to CO_2 adsorption. However, their contributions to CO_2 uptake capacity of ALPs would be negligible due to the much lower concentration of terminal amines compared to that of azo groups.

3.3Selective CO_2 capture over N_2 and CH_4

Because of their high Q_{st} for CO_2, narrow pore size, and moderate surface area, we expected high CO_2/N_2 and CO_2/CH_4 selectivity values for the new ALPs. To study the selective carbon dioxide capture over nitrogen and methane, single component CO_2, CH_4 and N_2 isotherms were collected at 273 and 298 K (Fig. 4 and S18).The adsorption behaviour of gas mixtures in porous materials can be predicted from single-component gas isotherms by the ideal adsorbed solution theory (IAST) method that predicts the selectivity values of porous sorbents as a function of the total pressure of gas mixtures.[16]Previous studies have shown that the IAST can provide a good prediction of gas mixtures adsorption behaviour in many zeolites and MOFs.[37] Furthermore, IAST has been widely used to predict CO_2/N_2 and CO_2/CH_4selectivity of many POPs using gas mixture composition similar to those of flue gas, natural gas, and landfill gas.[38-44]Therefore, we calculated CO_2/N_2 and CO_2/CH_4 selectivities for flue gas (CO_2:N_2 = 10:90) and landfill gas (CO_2:CH_4 = 50:50), as depicted in Fig. 5. Table 2 compares the selectivity values of new ALPs with those of ALP-1, which has the highest surface area and CO_2 uptake capacity among all classes of azo-linked POPs.

As seen in Table 2, all new ALPs have higher CO_2/N_2 and CO_2/CH_4 selectivity values than ALP-1.This can be due to their lower surface area and narrower pores which result in lower N_2 uptake compared to ALP-1.[9, 32]At 298K, the CO_2/N_2 selectivities of new ALPs (44-56) reach higher values than those of azo-POFs (37-42)[11]and are comparable to those of BILPs (31-57)[31] and functionalized NPOFs (38-59)[45].

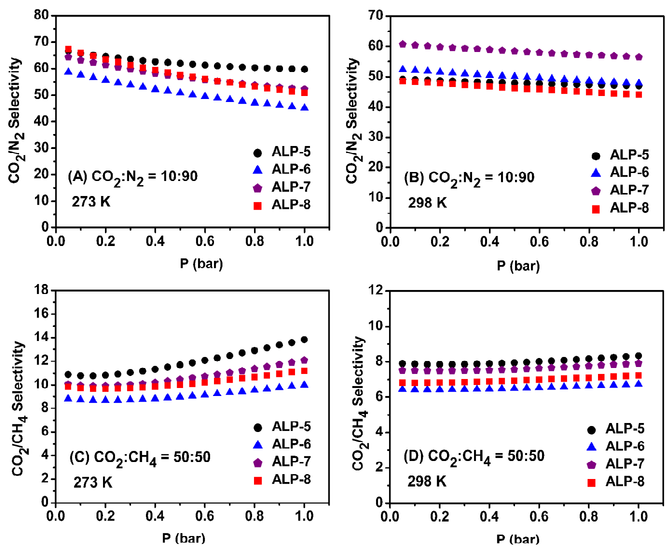

Fig. 5 IAST CO_2/N_2 selectivity of ALPs for CO_2:N_2 molar ratio of 10:90 at 273 K (A) and 298 K (B), and IAST CO_2/CH_4 selectivity of ALPs for CO_2:CH_4 molar ratio of 50:50 at 273 K (C) and 298 K (D).

At 273 K, ALP-5 shows the highest CO_2/N_2 and CO_2/CH_4 selectivities among all ALPs (Table 2). This can be attributed to its high Q_{st} for CO_2 which leads to high CO_2 uptakeat low pressures. In general, porous polymers with high $Q_{st}$for CO_2 show higherCO_2uptake capacity and selectivity.[3]ALP-7 shows high CO_2/N_2selectivity of 56 at 298 K, outperforming all other ALPs. This originates from the low surface area of ALP-7 which leads to very low N_2 uptake at 298 K.[3]These results are consistent with our previous findings that the structural characteristics (e.g. pore size, surface area, and pore volume) of azo-linked porous polymers play important roles in their performance in selective CO_2 capture.[9, 11]The higher porosity levels in POPs leads to enhanced CO_2 uptake capacities while the CO_2/N_2 selectivity values decrease with increasing surface area.[9] Generally, there is a trade-off between CO_2 uptake capacity and CO_2/N_2 selectivity, that is, porous materials having high CO_2 uptake capacity exhibit lower selectivity values than those with low CO_2 uptake capacity although this trend is not always followed by all materials.[3]Additionally, the nitrogen content of ALP-7 (16.46 wt. %) is higher than those of other ALPs (9.51-14.66 wt. %) which can contribute to the high CO_2/N_2 selectivity of ALP-7 at 298 K. Due to dipole-quadrupole interactions between CO_2 and nitrogen atoms, nitrogen-rich POPs generally exhibit high CO_2/N_2 selectivity values.[46]The CO_2/N_2 selectivities of new ALPs (44-56 at 298K) are lower than those of azo-COPs (96-131, 298K)[10] due to larger size of the pores in ALPs.[9]It is worth noting that azo-COP-2 which has the smallest pore size (~0.5 nm) among azo-COPs, outperforms other azo-COPs in CO_2/N_2selectivity.[10]Moreover, the high CO_2/N_2 of azo-COPs[10, 12] at 298 K has been explained by the new concept of nitrogen-phobicity,[10, 47-48] which is the enhancement in CO_2/N_2 selectivity values upon rise in adsorption temperature.While azo-COPs[10] show enhanced CO_2/N_2 selectivities at higher adsorption temperatures, the selectivities of ALPs decrease or remain almost constant upon increasing temperature (Table S5). This inconsistency can be attributed to the differences in porosity parameters of ALPs and azo-COPs. In fact, we and others have recently shown that the nitrogen-phobicity of porous polymers can be due to the physical nature of the pores rather than their chemical nature.[9, 47-48] Several studies have shown that porous polymers having the same functional groups but different porosity parameters can exhibit different behaviors in terms of N_2-phobicity.[9, 47-48] Very recently, Choi *et al.* have shown that the N_2-phobicity in porous polymers originates from the relatively large portion of mesoporosity in polymers.[48] Their results suggest that the N_2 uptake capacity of materials having larger mesopore portions decrease significantly upon raisingadsorption temperature.[48] This leads to enhanced CO_2/N_2 selectivity values at higher temperatures.[48]These findings can explain the different behavior of ALPs and azo-COPs[10] in terms of the change in CO_2/N_2 selectivities with adsorption temperature. As evidenced by their N_2 isotherms at 77 K, azo-COPs[10] have relatively large portion of mesopores while ALPs have lower degree of mesoporosity which leads to a gradual increase in Ar uptake at P/P_o = 0.04-0.90. Another study by Lu and Zhang reported the synthesis of azo-POFs via Zn-induced reductive homocoupling of aromatic nitro monomers and studied their performance in selective CO_2 capture.[11]Similar to ALPs; azo-POFs[11] exhibit lowered CO_2/N_2 selectivities upon rise in adsorption temperature, confirming the role of porosity parameters on the N_2-phobicity behavior of these polymers (Table S5). The surface area of azo-POFs (440-710 $m^2\ g^{-1}$)[11] are much lower than that of ALP-1 (1240 $m^2\ g^{-1}$)[9]; and therefore, azo-POFs have much lower CO_2 uptake capacities (1.2- 1.9 mmol g^{-1}, 298 K and 1 bar) than ALP-1 (3.2 mmol g^{-1}, 298 K and 1 bar). As expected, azo-POFs show higher CO_2/N_2 selectivity (37-42, 298 K)[11] values than ALP-1 (28, 298 K), further supporting our finding that CO_2/N_2 selectivity of azo-linked porous polymers depends on the structural characteristics of this class of materials.[9]The IAST CO_2/CH_4 selectivity of new ALPs was found to be 11-14 at 273 K which decreases to 7-8 at 298 K. ALP-5 shows the highest CO_2/CH_4 selectivity values among all ALPs during the entire loading (Fig. 5), due to its high Q_{st} for CO_2. The CO_2/CH_4 selectivities of ALPs are much lower than CO_2/N_2 selectivity values. This is due to higher CH_4 uptakes of ALPs compared to their N_2 uptakes, which originates fromthe higher polarizability of CH_4 (26×10^{-25} cm^3) than that of N_2 (17.6×10^{-25} cm^3).[49]We also calculated the selectivities of ALPs by initial slope method using the ratios of Henry's law constants (Fig. S27-S30). Consistent with IAST studies, all new ALPs show higher initial slope CO_2/N_2 selectivity values than ALP-1 (Table S6). This can attributed to lower surface areas and narrower pores of new ALPs.[3]

3.4 Evaluation of ALPs for PSA and VSA processes

For comprehensiveevaluation of porous adsorbents for VSA and PSA processes, five criteria have been recently developed by Bae and Snurr,[16]which aredefined in the following and summarized in Table 3. *CO_2 uptake under adsorption conditions* (N_1^{ads}) is defined as the CO_2 uptake capacity of the sorbent when the partial pressure of CO_2 in a binary gas mixture is taken into account.*Working CO_2 capacity (ΔN_1)*, defined as $\Delta N_1 = N_1^{ads} - N_1^{des}$, shows the difference between CO_2 uptake capacity at the adsorption pressure (N_1^{ads}) and the desorption pressure (N_1^{des}) when the partial pressure of CO_2 in a binary gas mixture is considered.*Regenerability (R),* which is defined as $R = (\Delta N_1/N_1^{ads}) \times 100$ %, shows the percentage of adsorption sites that can be regenerated upon lowering the pressure during the desorption step.S*electivity under adsorption conditions* (α_{12}^{ads}) is defined as $(\alpha_{12}^{ads}) = (N_1^{ads}/N_2^{ads}) \times (y_2/y_1)$, where N ^{ads} and y are the adsorbed amount and the mole fraction of each component in a binary gas mixture respectively, subscripts 1 and 2 indicate the strongly adsorbed component (CO_2) and the weakly adsorbed component (CH_4 or N_2) respectively. *Sorbent selection parameter (S)* is defined as $S=(\alpha_{12}^{ads})^2/(\alpha_{12}^{des}) \times (\Delta N_1/\Delta N_2)$ where superscripts ads and des represent the adsorption and desorption conditions, respectively. The *S* value combines the selectivity values at adsorption and desorption pressures with working capacity of both components of the gas mixture. It is noteworthy that none of these criteria are perfect, but they are complementary; and therefore, these criteria must be considered together for a comprehensive evaluation of sorbents.[16] These criteria reflect the performance of sorbents under equilibrium conditions and do not take into account the kinetics of adsorption and desorption processes. The experimental setup for measurement of gas mixture adsorption is complicated; and therefore, to calculate the evaluation criteria, IAST is usually used to predict the behaviour of a binary gas mixture from single-component isotherms.[16] As such, we used IAST to assess the performance of ALPs for CO_2 separation from flue gas and landfill gas by VSA and PSA. The evaluation criteria of ALPs were calculated from CO_2, CH_4, and N_2 adsorption isotherms collected at 298 K (Fig. S18, S25, and S26).

Table 3 Adsorbent evaluation criteria[a]

CO_2 uptake under adsorption conditions (mol kg^{-1})	N_1^{ads}
Working CO_2 capacity (mol kg^{-1}), $N_1^{ads} - N_1^{des}$	ΔN_1
Regenerability (%), $(\Delta N_1/N_1^{ads}) \times 100$ %	**R**
Selectivity under adsorption conditions, $(N_1^{ads}/N_2^{ads}) \times (y_2/y_1)$	α_{12}^{ads}
Sorbent selection parameter, $(\alpha_{12}^{ads})^2/(\alpha_{12}^{des}) \times (\Delta N_1/\Delta N_2)$	S

[a]N: adsorbed amount. y: mole fraction in gas mixture. Subscripts 1 and 2 indicate the strongly adsorbed component (CO_2) and the weakly adsorbed component (CH_4 or N_2), respectively. Superscripts "ads" and "des" refer to adsorption and desorption conditions, respectively. α_{12}: selectivity of component 1 over component 2.

3.4.1 CO_2 separation from flue gas using VSA

To evaluate the performance of ALPs in CO_2 separation from flue gas, the CO_2:N_2 mole ratio was assumed to be 10:90. The evaluation criteria were calculated by setting the adsorption pressure (P^{ads}) and desorption pressure (P^{des}) to 1.0 bar and 0.1bar, respectively. Table 4 compares the performance of ALPs with those of different classes of promising porous sorbents.As seen in Table 4, ALP-5 has the highest working capacity among all ALPs. This can be attributed to the combined effects of its high Q_{st} for CO_2 and relatively high surface area.[16]Interestingly, although the surface area of ALP-5 (801 m^2 g^{-1}) is much lower than that of ALP-1 (1235 m^2 g^{-1}), it hasa higher working capacity than ALP-1 (Table 4). This can be attributed to thehigher Q_{st} of ALP-5 for CO_2which results in higher CO_2 uptake at low pressures.[16] Other ALPs (ALP-6, -7, -8) have relatively low working capacities due to their low surface areas which lead to low CO_2 uptakes.The working capacity of ALP-5 (0.63) surpasses those of previously reported POPs such as BILPs (0.30-0.49)[31], SNU-Cls (0.41- 0.51)[50], and TBILPs (0.35- 0.59)[51]. On the other hand, Ni-MOF-74 and Zeolite-13X have higher working capacities than ALP-5 due to their higher $Q_{st}$for CO_2(~38 kJ mol^{-1}). It is worth mentioning that the high Q_{st}values of Ni-MOF-74 and Zeolite-13X for CO_2 result in low regenerability levels (Table 4).[17]In addition, Ni-MOF-74 and Zeolite-13X have much lower S values than ALP-5 due to their high working capacity for nitrogen (ΔN_2).

Table 4 VSA evaluation criteria for CO_2 separation from flue gas[a]

Adsorbents	N_1^{ads}	ΔN_1	R	α_{12}^{ads}	S
ALP-1[9]	0.57	0.51	88.6	28.0	85.2
ALP-5	0.72	0.63	87.4	47.0	233.7
ALP-6	0.41	0.36	88.1	47.7	228.7
ALP-7	0.32	0.28	87.9	56.4	326.8
ALP-8	0.38	0.33	88.0	44.1	195.2
BILP-12[31]	0.55	0.49	88.7	27.1	72.6
TBILP-2[51]	0.67	0.59	88.3	42.1	192.3
SNU-Cl-sca[50]	0.58	0.51	88.5	17.0	88
ZIF-78[16]	0.60	0.58	96.3	34.5	396
HKUST-1[16]	0.62	0.55	89.0	20.4	46.2
Ni-MOF-74[16]	4.34	3.2	73.7	41.1	83.5
Zeolite-13X[16]	2.49	1.35	54.2	86.2	128

[a]CO_2:N_2= 10:90, T= 298K, P^{ads}= 1 bar, and P^{des} = 0.1 bar.

3.4.2 CO_2 separation from landfill gas using VSA

While landfill gas is an important source of CH_4, it consists of approximately 40-60% CO_2.[17] This significant level of CO_2 results in low energy density of the fuel and also corrosion of pipelines and tanks used for transportation of CH_4.[52] Therefore, CO_2separation from landfill gas is necessary before transportation and storage.[17, 53]To assess the performance of ALPs in CO_2 separation from landfill gas, we assumed the CO_2:CH_4 mole ratio to be 50:50 and set the adsorption and desorption pressure to 1 and 0.1bar, respectively. As seen in Table 5, ALP-1 shows the highest working capacity among ALPs due to its higher surface area.[31]On the other hand,the working capacity of ALP-1 for separation of CO_2 from flue under VSA process is lower than that of ALP-5 despite its higher surface area (Table 4). It can be concluded that the effect of surface area on working capacity becomes more dominant when the partial pressure of CO_2 in binary gas mixtures increases.[16, 31]ALP-5 has the highest$S$ value among all adsorbents listed in Table 5, due to its high working capacity for CO_2, high CO_2/CH_4 selectivity, and low working capacity for CH_4. ALP-5 outperforms previously reported POPs such as BILPs,[31] SNU-C1s,[50] and TBILPs[51]considering all evaluation criteria together for CO_2 separation from landfill gas by VSA. Due to their moderate Q_{st} for CO_2 (29.2-32.5 kJ mol^{-1}), ALPs have high regenerability values of 81-85%, while adsorbents such as Ni-MOF-74 and Zelolite-13X which have high Q_{st} for CO_2(~38 kJ mol^{-1}) exhibit much lower regenerabilities of ~ 50% (Table 5).[16]

Table 5 VSA evaluation criteria for CO_2 separation from landfill gas[a]

Adsorbents	N_1^{ads}	ΔN_1	R	α_{12}^{ads}	S
ALP-1[9]	2.04	1.73	85.1	5.8	35.1
ALP-5	2.07	1.67	80.9	8.3	75.0
ALP-6	1.40	1.17	84.0	6.7	47.9
ALP-7	1.04	0.86	83.0	7.9	66.9
ALP-8	1.29	1.08	83.8	7.2	56.2
BILP-12[31]	2.01	1.71	85.3	6.0	33.7
TBILP-2[51]	2.20	1.84	83.7	7.6	62.5
SNU-Cl-sca[50]	1.99	1.60	80.4	7.5	38
ZIF-82[16]	1.42	1.20	84.9	5.6	20.5
HKUST-1[16]	2.81	1.90	67.5	5.5	19.8
Ni-MOF-74[16]	6.23	3.16	50.7	8.5	21.0
Zeolite-13X[16]	3.97	1.97	49.6	13.2	19.1

[a]CO_2:CH_4= 50:50, T= 298K, P^{ads}= 1 bar, and P^{des} = 0.1 bar.

3.4.3 CO_2 separation from landfill gas using PSA

For PSA processes, high surface area adsorbents are more promising than those having low or moderate surface areas.[17, 31]Therefore, we have only evaluated the performance ofALP-1 and ALP-5 for CO_2 separation from landfill gas using PSA since both polymers have higher surface area than other ALPs. The CO_2:CH_4 mole ratio wasassumed to be 50:50, and the adsorption and desorption pressureswere set to 5 and 1 bar, respectively.The PSA evaluation criteria of ALPs for separation of CO_2 from landfill gas are summarized and compared with those of different classes of adsorbents in Table 6. Most notably,ALP-5 has the highest CO_2/CH_4 selectivity under adsorption conditions (α_{12}^{ads}) and also the highest S value among all materials listed in Table 6. ALP-5 has lower working capacity than ALP-1, which can be attributed to its lower surface area and pore volume. Consistently, ALP-5 exhibits relatively low working capacity when compared to other POPs of higher surface area such as BILP-12[31] and TBILP-2[51] (1080-1479 m^2 g^{-1}).It is important to note that ALP-5 has high working capacities for VSA processes compared to other POPs (Tables 4 and 5); however, it has a low working capacity under PSA process when compared to other POPs such as BILP-12 and TBILP-2 (Table 6).

Table 6. PSA evaluation criteria for CO_2 separation from landfill gas[a]

Adsorbents	N_1^{ads}	ΔN_1	R	α_{12}^{ads}	S
ALP-1[9]	4.27	2.49	58.2	6.8	38.3
ALP-5	3.22	1.68	52.3	9.0	46.5
BILP-12[31]	5.04	3.02	59.8	5.8	29.7
TBILP-2[51]	4.28	2.32	54.33	7.2	31.9
HKUST-1[16]	8.01	5.34	66.7	4.9	21.0
Ni-MOF-74[16]	8.48	2.25	26.5	2.93	1.05
Zeolite-13X[16]	5.37	1.40	26.1	4.2	2.0

[a]CO_2:CH_4= 50:50, T= 298K, P^{ads}= 5 bar, and P^{des} = 1 bar.

This is consistent with previous findings that oneCO_2 adsorbent cannot simultaneously beoptimized for all VSA and PSA processes.[16-17]In general, CO_2adsorbents with moderate surface area and high Q_{st} for CO_2 are more favourable for VSA processes; however, high surface area adsorbents with moderate Q_{st} for CO_2 are more efficient for PSA applications.[16, 31]Consistently, although Ni-MOF-74 and zeolite-13X are very promising candidates for CO_2 separation by VSA processes (Table 4 and 5), they have very low working capacities for separation of CO_2 from landfill gas by PSA (Table 6) due to their high Q_{st} for CO_2(~ 38 kJ mol^{-1}). On the other hand, HKUST-1 with a lower working capacities than Ni-MOF-74 and zeolite-13X for VSA processes, outperforms Ni-MOF-74 and zeolite-13X for separation of CO_2 from landfill gas by PSA due to its high surface area (1570 m^2 g^{-1}) and moderate Q_{st} for CO_2 (29 kJ mol^{-1}). Because of its high surface area, ALP-1 has high working capacity of 2.49 mol kg^{-1}, which is comparable to those of the best benzimidazole-linked polymers such as BILP-12 and TBILP-2 (Table 6).

4 Conclusions

We have synthesized four new porous azo-linked polymers (ALPs) and studied their performance in selective CO_2 capture over N_2 and CH_4.The CO_2 uptake capacity of ALPs is influenced by their surface area and Q_{st} value for CO_2. At very low pressures, the CO_2 uptake correlates more with Q_{st} for CO_2, while the CO_2 uptake at high pressuresis more dependent on the surface area. One of the polymers, ALP-5, exhibits high $Q_{st}$for CO_2 (32.5 kJ mol^{-1}) which is the highest Q_{st} value among all reported azo-linked porous polymers.At 1 bar, ALP-5 shows CO_2 uptake capacities of 4.46 and 2.94 mmol g^{-1} at 273 and 298 K, respectively. This high uptake is due to high surface area and high Q_{st} for CO_2.At 298 K, all ALPs have high selectivities for CO_2/N_2(44-56) but moderate selectivity for CO_2/CH_4(7-8). Moreover, the CO_2 separation ability of ALPs from flue gas and landfill gas under VSA and PSA conditions was found to be influenced by surface area of ALPs and their Q_{st} for CO_2.The overall results show that ALPs which have moderate surface area and high Q_{st} for CO_2 are more favourable for VSA processes; whereas, ALPs having high surface area and moderate Q_{st} for CO_2 perform better in PSA applications.The evaluation of ALPs for CO_2 separation from flue gas and landfill gas revealed that ALPs are among the most promising porous organic polymers for VSA and PSA processes.

Acknowledgements

This work was supported by the U.S. Department of Energy, Office of Basic Energy Sciences, Division of Materials Sciences and Engineering under award number (DE-SC0002576).

Notes and references

Department of Chemistry, Virginia Commonwealth University, Richmond, VA 23284-2006, United States. Fax: +1 804 828 8599; Tel: +1 804 828 7505; E-mail: helkaderi@vcu.edu

Electronic Supplementary Information (ESI) available: characterization of porous networks and their gas uptake and selectivity studies.See DOI: 10.1039/b000000x/

1. X. Zou, H. Ren and G. Zhu, *Chem. Commun.*, 2013, **49**, 3925-3936.
2. Y. Xu, S. Jin, H. Xu, A. Nagai and D. Jiang, *Chem. Soc. Rev.*, 2013, **42**, 8012-8031.
3. R. Dawson, A. I. Cooper and D. J. Adams, *Polym. Int.*, 2013, **62**, 345-352.
4. J.-R. Li, Y. Ma, M. C. McCarthy, J. Sculley, J. Yu, H.-K. Jeong, P. B. Balbuena and H.-C. Zhou, *Coord. Chem. Rev.*, 2011, **255**, 1791-1823.
5. G. T. Rochelle, *Science*, 2009, **325**, 1652-1654.
6. K. Sumida, D. L. Rogow, J. A. Mason, T. M. McDonald, E. D. Bloch, Z. R. Herm, T.-H. Bae and J. R. Long, *Chem. Rev.*, 2011, **112**, 724-781.
7. M. Nandi and H. Uyama, *Chem. Rec.*, 2014, **14**, 1134-1148.
8. B. Ashourirad, A. K. Sekizkardes, S. Altarawneh and H. M. El-Kaderi, *Chem. Mater.*, 2015, **27**, 1349-1358.
9. P. Arab, M. G. Rabbani, A. K. Sekizkardes, T. İslamoğlu and H. M. El-Kaderi, *Chem. Mater.*, 2014, **26**, 1385-1392.
10. H. A. Patel, S. H. Je, J. Park, D. P. Chen, Y. Jung, C. T. Yavuz and A. Coskun, *Nat. Commun.*, 2013, **4**, 1357.
11. J. Lu and J. Zhang, *J. Mater. Chem. A.*, 2014, **2**, 13831-13834.
12. H. A. Patel, S. H. Je, J. Park, Y. Jung, A. Coskun and C. T. Yavuz, *Chem. Eur. J.*, 2014, **20**, 772-780.
13. C. M. Nagaraja, R. Haldar, T. K. Maji and C. N. R. Rao, *Cryst. Growth Des.*, 2012, **12**, 975-981.
14. J. Park, D. Yuan, K. T. Pham, J.-R. Li, A. Yakovenko and H.-C. Zhou, *J. Am. Chem. Soc.*, 2012, **134**, 99-102.
15. S. Wu, Y. Liu, G. Yu, J. Guan, C. Pan, Y. Du, X. Xiong and Z. Wang, *Macromolecules*, 2014, **47**, 2875-2882.
16. Y.-S. Bae and R. Q. Snurr, *Angew. Chem. Int. Ed.*, 2011, **50**, 11586-11596.
17. C. E. Wilmer, O. K. Farha, Y.-S. Bae, J. T. Hupp and R. Q. Snurr, *Energy Environ. Sci.*, 2012, **5**, 9849-9856.
18. S.-Y. Moon, H.-R. Mo, M.-K. Ahn, J.-S. Bae, E. Jeon and J.-W. Park, *J. Polym. Sci., Part A: Polym. Chem.*, 2013, **51**, 1758-1766.
19. K. Xu and J. Economy, *Macromolecules*, 2004, **37**, 4146-4155.
20. F. Sun, G. Zhang, D. Zhang, L. Xue and H. Jiang, *Org. Lett.*, 2011, **13**, 6378-6381.
21. S. Ma and H.-C. Zhou, *Chem. Commun.*, 2010, **46**, 44-53.
22. D. E. Demirocak, M. K. Ram, S. S. Srinivasan, D. Y. Goswami and E. K. Stefanakos, *J. Mater. Chem. A.*, 2013, **1**, 13800-13806.
23. P. Kaur, J. T. Hupp and S. T. Nguyen, *ACS Catal.*, 2011, **1**, 819-835.
24. C. Shen, Y. Bao and Z. Wang, *Chem. Commun.*, 2013, **49**, 3321-3323.
25. F. M. Wisser, K. Eckhardt, D. Wisser, W. Böhlmann, J. Grothe, E. Brunner and S. Kaskel, *Macromolecules*, 2014, **47**, 4210-4216.
26. X. Feng, X. Ding and D. Jiang, *Chem. Soc. Rev.*, 2012, **41**, 6010-6022.
27. X. Zhang, J. Lu and J. Zhang, *Chem. Mater.*, 2014, **26**, 4023-4029.
28. W. Lu, Z. Wei, D. Yuan, J. Tian, S. Fordham and H.-C. Zhou, *Chem. Mater.*, 2014, **26**, 4589-4597.
29. T. Ben, Y. Li, L. Zhu, D. Zhang, D. Cao, Z. Xiang, X. Yao and S. Qiu, *Energy Environ. Sci.*, 2012, **5**, 8370-8376.
30. H. Ma, H. Ren, X. Zou, S. Meng, F. Sun and G. Zhu, *Polym. Chem.*, 2014, **5**, 144-152.
31. A. K. Sekizkardes, T. Islamoglu, Z. Kahveci and H. M. El-Kaderi, *J. Mater. Chem. A.*, 2014.
32. G. Li, B. Zhang, J. Yan and Z. Wang, *Macromolecules*, 2014, **47**, 6664-6670.
33. P. Arab, A. Verlander and H. M. El-Kaderi, *J. Phys. Chem. C.*, 2015, **119**, 8174-8182.
34. W. Lu, D. Yuan, J. Sculley, D. Zhao, R. Krishna and H.-C. Zhou, *J. Am. Chem. Soc.*, 2011, **133**, 18126-18129.
35. S. Sung and M. P. Suh, *J. Mater. Chem. A.*, 2014, **2**, 13245-13249.
36. W.-C. Song, X.-K. Xu, Q. Chen, Z.-Z. Zhuang and X.-H. Bu, *Polym. Chem.*, 2013, **4**, 4690-4696.
37. B. Liu and B. Smit, *Langmuir*, 2009, **25**, 5918-5926.
38. Y. Byun and A. Coskun, *Chem. Mater.*, 2015, **27**, 2576-2583.
39. H. A. Patel, D. Ko and C. T. Yavuz, *Chem. Mater.*, 2014, **26**, 6729-6733.
40. G. Li and Z. Wang, *J. Phys. Chem. C.*, 2013, **117**, 24428-24437.
41. G. Liu, Y. Wang, C. Shen, Z. Ju and D. Yuan, *J. Mater. Chem. A.*, 2015, **3**, 3051-3058.
42. X. Zhu, S. M. Mahurin, S.-H. An, C.-L. Do-Thanh, C. Tian, Y. Li, L. W. Gill, E. W. Hagaman, Z. Bian, J.-H. Zhou, J. Hu, H. Liu and S. Dai, *Chem. Commun.*, 2014, **50**, 7933-7936.
43. Y. Liao, J. Weber and C. F. J. Faul, *Macromolecules*, 2015.
44. M. Saleh and K. S. Kim, *R. Soc. Chem. Adv.*, 2015, **5**, 41745-41750.
45. T. Islamoglu, M. Gulam Rabbani and H. M. El-Kaderi, *J. Mater. Chem. A.*, 2013, **1**, 10259-10266.
46. P.-Z. Li and Y. Zhao, *Chem. Asian J.*, 2013, **8**, 1680-1691.
47. M. Saleh, S. B. Baek, H. M. Lee and K. S. Kim, *J. Phys. Chem. C.*, 2015, **119**, 5395-5402.
48. J. H. Lee, H. J. Lee, S. Y. Lim, B. G. Kim and J. W. Choi, *J. Am. Chem. Soc.*, 2015.**137** , 7210-7216.
49. X.-M. Hu, Q. Chen, Y.-C. Zhao, B. W. Laursen and B.-H. Han, *J. Mater. Chem. A.*, 2014, **2**, 14201-14208.
50. L.-H. Xie and M. P. Suh, *Chem. Eur. J.*, 2013, **19**, 11590-11597.
51. A. K. Sekizkardes, S. Altarawneh, Z. Kahveci, T. I□slamog□lu and H. M. El-Kaderi, *Macromolecules*, 2014, **47**, 8328-8334.
52. O. K. Farha, Y.-S. Bae, B. G. Hauser, A. M. Spokoyny, R. Q. Snurr, C. A. Mirkin and J. T. Hupp, *Chem. Commun.*, 2010, **46**, 1056-1058.
53. Y.-S. Bae, B. G. Hauser, O. K. Farha, J. T. Hupp and R. Q. Snurr, *Microporous Mesoporous Mater.*, 2011, **141**, 231-235.

TOC

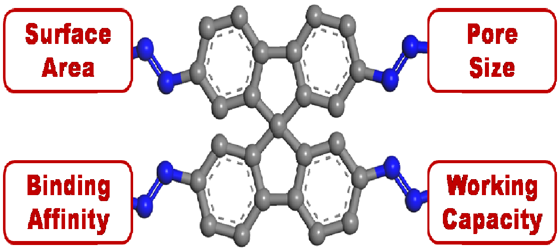

The correlation between the CO_2-capturing ability of porous azo-linked polymers and their structural properties was investigated.